

## CLAY SONIFICATION TOOL IN PROCESSING OF POLYPROPYLENE NANOCOMPOSITES FILMS

<sup>1</sup>Isabelle Berenguer, <sup>1\*</sup> Washington Luiz Oliani, <sup>1</sup>Luiz Gustavo Hiroki Komatsu,  
<sup>2,3</sup>Nilton Lincopan, <sup>4</sup>Vijaya Kumar Rangari, <sup>1</sup>Duclerc Fernandes Parra

<sup>1</sup>Nuclear and Energy Research Institute, IPEN-CNEN/SP, Av. Prof. Lineu Prestes, 2242, Cidade Universitária,  
CEP 05508-000, São Paulo – SP, Brazil  
\* [washoliani@usp.br](mailto:washoliani@usp.br)

<sup>2</sup>Department of Microbiology, Institute of Biomedical Sciences, University of Sao Paulo, CEP 05508-000, São  
Paulo, Brazil

<sup>3</sup>Department of Clinical Analysis, School of Pharmacy, University of Sao Paulo, São Paulo, Brazil

<sup>4</sup>Center for Advanced Materials Science and Engineering Tuskegee University, AL 36088, USA

### ABSTRACT

The aim this study was to use ultrasound mixing of clay particles to obtain nanocomposites of polypropylene. PP was modified by irradiation in acetylene at dose of 12.5 kGy, with montmorillonite (MMT) and silver nanoparticles (AgNPs), prepared by melt intercalation in a twin-screw extruder. As compatibilizer agent it has been used a polypropylene graft maleic anhydride (PP-g-MA) and surfactant agent oleic acid (AO). The AgNPs was formed by self-arrangement of the surfactant as a template under ultrasound radiation. The nanocomposites were evaluated by scanning electron microscopy and dispersive spectroscopy (SEM/EDX), FTIR spectroscopy, differential scanning calorimetry (DSC), X-Ray diffraction (XRD) and determination of antibacterial activity. The antibacterial activity of as-prepared films PP/AgNPs/MMT were tested against strains of two different groups of bacteria-*Staphylococcus aureus* (*S. aureus*; gram-positive bacteria) and *Escherichia coli* (*E. Coli*; gram-negative bacteria).

### 1. INTRODUCTION

Polyolefins, such as polyethylene (PE) and polypropylene (PP) are highly versatile thermoplastics because of their well-balanced physical and mechanical properties, good moisture stability and easy processability at a relatively low cost, which make them a versatile material with continuously increasing applications [1].

Polypropylene for the reason of its good process ability [2], cost competitiveness [3] and enormous applications on the industry have been focused on as one of most widely used commodity polymers [4]. However, PP has a linear structure, which means it has low melt strength and cannot be use in process that requires high stretch. For this case, to modify polypropylenes, several methods have been applied by the addition of long chain branches using irradiation [5].

Radiation effects on polypropylene crosslinking and main-chain scission in amorphous regions and main-chain scission in crystalline regions. The long-chain branching formation is enhanced by the melted state irradiation. The most significant improvement from radiation

induced LCB is on the rheological properties and hence the processability of the polymers, especially in *high melt strength polypropylene* HMSPP [6].

Barrier properties of PP nanocomposite with clay have attracted extensive attention, especially for industrial interest. The use of montmorillonite (MMT) clay has been extensively tested by other authors and its ability to increase properties of nonpolar polymers such as PP has been widely proven [7]. A limited reprocessing of PP/MMT materials can improve the intercalation/exfoliation of the clay in the PP matrix and hence optimized mechanical properties and clay morphology [8].

Nowadays nanocomposite formation represents an attractive route to upgrade and diversify well-known polymeric materials and to afford unique property profiles [9]. Surfaces with antibacterial properties are highly desired in applications that require a protective barrier against infection [10]. At present, many researchers have focused on antibacterial and multi-functional properties of silver nanoparticles [11]. Silver is particularly attractive because it combines a high toxicity for bacteria with a low toxicity for human [12]. The overall antibacterial effect of silver nanoparticles is related to particle size and shape and is highly dependent on particle dispersion. The presence of macro aggregates can lead to a decrease in antibacterial activity, so good particles is needed [13]. For this reason, surfactants are usually employed to reduce aggregate formation [14].

Different surfactants have been used in several projects. Although, interesting results have been obtained with poly(N-vinyl-2-pyrrolidone) and oleic acid (OA). In this present work, oleic acid was used as coating of silver nanoparticles to perform particle homogeneous dispersion [15].

The efficiency of the clay to modify the properties of the polymer is primarily determined by the degree of its dispersion in the polymer matrix which, in turn, depends on the clay particle size [16]. The complete dispersion of clay nanolayers in a polymer optimizes the number of available reinforcing elements that carry an applied load and deflect the evolving cracks [17].

In order to improve the affinity between the hydrophilic clay surface and the hydrophobic polymer chains, maleic anhydride grafted polypropylene (PP-g-MA) was used as compatibilizer [18]. The aim of this work is to produce nanocomposite films polypropylene via extrusion processing and assess the biocide activity.

## **2. EXPERIMENTAL**

### **2.1. Materials**

The isotactic Polypropylene (iPP) was supplied by Braskem – Brazil in pellets with MFI= 1.5 dg min<sup>-1</sup> and Mw= 338,000 g mol<sup>-1</sup>. The acetylene 99.8% supplied by White Martins S/A, of Brazil, was used to synthesis of modified polypropylene. Silver nanoparticles (AgNPs) were purchased from Sigma Aldrich; oleic acid (AO) was supplied by Labsynth. The commercial nanoclay CLOISITE 20 was provided by BYK Additives Company; IRGANOX by Ciba and compatibilizer agent, propylene maleic anhydride graft copolymer (PP-g-MA) was supplied by Addivant (Polybond 3200).

## 2.2. Methods

### 2.2.1. Radiation process

The irradiation of the pellets was performed under acetylene atmosphere in a  $^{60}\text{Co}$  gamma source at dose rate of  $5 \text{ kGy h}^{-1}$ . The polypropylene irradiation was performed at  $12.5 \text{ kGy}$  dose monitored by a Harwell Red Perspex 4034 dosimeter. After irradiation, the samples were heated for 1h at  $90 \text{ }^\circ\text{C}$  to promote the recombination and annihilation of residual radicals [19, 20]. Two different formulations containing the polypropylene were prepared and are represented in Table 1.

**Table 1: Formulations of the samples.**

Samples	Matrix	Dose/ kGy	PP-g-MA /wt%	Irganox/wt %	Cloisite 20 /wt%	AgNPs/ wt%	AO/ wt%
PP1	HMSPP	12.5	-	2	-	-	-
PP2	HMSPP	12.5	2	2	1	0.1	10

### 2.3. Preparations of the PP-MMT-AgNPs Nanocomposite Films

A Unique ultrasound equipment model USC-1400, with a working frequency of 40 kHz and maximum intensity output of 135 watts was used to deagglomerate the silver nanoparticles in oleic acid solution. The HMSPP 12.5 kGy in pellet was mixed with Irganox B 215 ED and PP-g-MA in a rotary mixer and maintained under this condition for 24 hours. Then the mixture was processed with the addition of clay (MMT 1% by weight) and silver nanoparticles (AgNPs 0.1% by weight) in a twin-screw extruder Haake co-rotating, model Rheomex PTW 16/25, with the following processing conditions: the temperature profile (feed to die) was  $175\text{-}230 \text{ }^\circ\text{C}$ , with a speed of 100 rpm. After processed, the nanocomposites were granulated in a granulator Primotécnica W-702-3. The PP/MMT-AgNPs films were produced in blow extruder and the material was placed directly into the hopper of the extruder with a temperature profile (feed to die) of  $175\text{-}220 \text{ }^\circ\text{C}$ , screw speed of 20 rpm and torque of 31-40 Nm. The films were produced with a thickness of  $\sim 0.05 \text{ mm}$ .

#### 2.3.1. Scanning electron microscopy and dispersive spectroscopy

Scanning electron microscopy was done using an EDAX PHILIPS XL 30. In this project, thin coat of carbon was sputter coated onto the samples.

#### 2.3.2. Fourier transformed infrared spectroscopy

The analyses were performed using attenuation total reflectance accessory (ATR) transmittance in the Thermo Nicolet spectrophotometer, model 380 FT-IR.

#### 2.3.3. Differential scanning calorimetry

Thermal properties of specimens were analyzed using a differential scanning calorimeter DSC 822, Mettler Toledo. The thermal behavior of films was obtained by (1) heating from  $25$  to  $280 \text{ }^\circ\text{C}$  at a heating rate of  $10 \text{ }^\circ\text{C min}^{-1}$  under nitrogen atmosphere; (2) holding for 5 min at  $280 \text{ }^\circ\text{C}$ ; and (3) then cooling to  $25 \text{ }^\circ\text{C}$  and reheating to  $280 \text{ }^\circ\text{C}$  at  $10 \text{ }^\circ\text{C min}^{-1}$ .

### 2.3.4. X-ray diffraction

X-ray diffraction measurements were carried out in the reflection mode on a Rigaku diffractometer Mini Flex II (Tokyo, Japan) operated at 30 kV voltage and current of 15 mA with CuK $\alpha$  radiation ( $\lambda = 1,541841 \text{ \AA}$ ).

### 2.3.5. Determination of antibacterial activity

An aliquot (400  $\mu\text{L}$ ) of a cell suspension of either *Staphylococcus aureus* ATCC 27853 ( $10^6$  cells  $\text{mL}^{-1}$ ) or *Escherichia coli* ATCC 25922 ( $10^6$  cells  $\text{mL}^{-1}$ ) prepared using the method described in JIS Z 2801 [21] were held in intimate contact with each of the 2 replicates of the test surfaces supplied using a 45 x 45  $\text{mm}^2$  polypropylene film for 24 hours at 37 °C under humid conditions. The size of the surviving population was determined using a method based on JIS Z 2801. The viable cells in the suspension were enumerated by viable cell counts on MacConkey Agar after incubation at 37 °C for 24 hours using a 100  $\mu\text{L}$  sample taken from the test surfaces.

## 3. RESULTS AND DISCUSSION

### 3.1. Scanning electron microscopy and dispersive spectroscopy

The result determined by SEM and EDX is observed in the picture bellow, Fig.1.

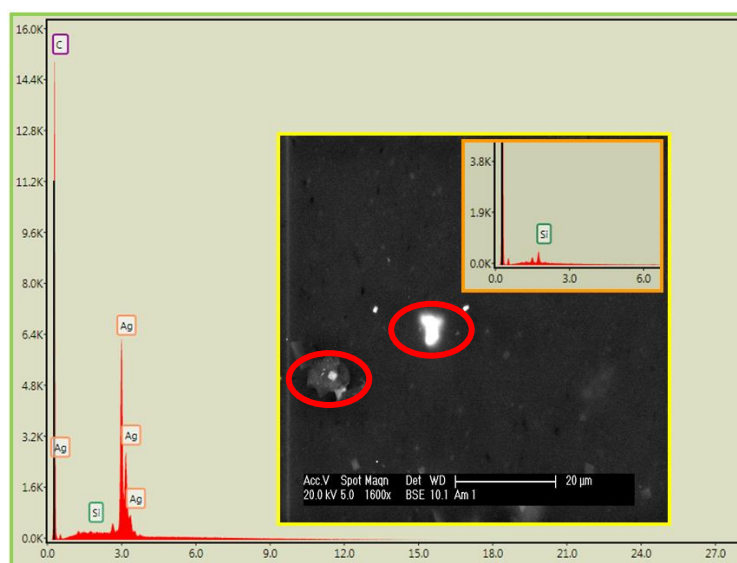


**Figure 1: SEM image and EDX of the PP2 nanocomposite film.**

The polypropylene nanocomposite film, Fig.1, there is a micrometer aggregates clay and the incidence of nanosilver, characterized by EDX. Larger particles (encircled) were observed which can be attributed to inhomogeneous dispersion of clay particles in PP matrix due to their inherent incompatibility.

### 3.2. Fourier transformed infrared spectroscopy

Fig. 2 shows the infrared spectrum of the samples PP1 and PP2.

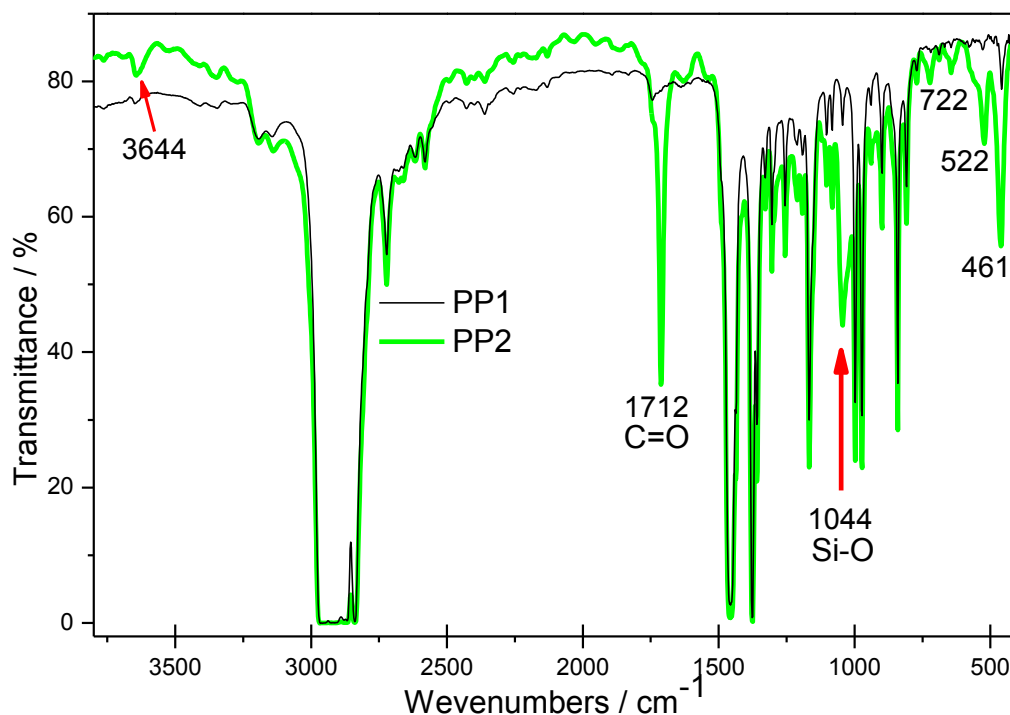


**Figure 2: Illustration of the FTIR spectra of films polypropylene**

The infra-red spectroscopy, IR, is the versatile method to follow chemical modifications in a polymeric material. The band attributed to stretching of the carbonylic group C=O, appears in the IR spectrum as an intense band, at around  $1712\text{ cm}^{-1}$ , as observed in the Fig. 2. However, a weak sample had shown in the IR spectrum of modified PP at around  $1044\text{ cm}^{-1}$ . This band was Si-O. Furthermore, there is an intense band at around  $3644\text{ cm}^{-1}$ . According to the literature [22], the carbonyl band appears at  $1711\text{ cm}^{-1}$ . The broad feature from 3500 to 2500 is characteristic of the O–H stretching band of the acid which is known to be in dimeric form due to hydrogen bonding.

### 3.3. Differential scanning calorimetry

The DSC results for PP1 and PP2 are presented in Table 2 and Fig. 3.

**Table 2: Sample values of melting peak temperature, melt-crystallization temperature and degree of crystallinity**

Samples	Melting peak temperature, $T_{m1}$ /°C ( $\pm 0.1\%$ )	Crystallization peak temperature, $T_c$ /°C ( $\pm 0.1\%$ )	Melting peak temperature, $T_{m2}$ /°C ( $\pm 0.1\%$ )	Degree of crystallinity, $X_c$ /% ( $\pm 0.5\%$ )
PP1	164.6	127.8	163.6	48.4
PP2	163.2	124.1	162.0	44.7

The DSC curves corresponding to PP1 and PP2 showed one melting peak at  $164.6\text{ }^\circ\text{C}$  and  $163.2\text{ }^\circ\text{C}$ , respectively. In terms of crystallinity, the sample one showed a peak at  $127.8\text{ }^\circ\text{C}$  and sample two a peak at  $124.1\text{ }^\circ\text{C}$ . Another melting peak is observed at  $163.6\text{ }^\circ\text{C}$  for sample one and  $162.0\text{ }^\circ\text{C}$  for PP2. In Table 2, the degree of crystallinity it is very intense, from 48.4% to 44.7%. According to the literature [23], the value of  $X_c$  decreases with increasing

the content of clay, indicating that the nanocomposites can achieve the same degree of crystallinity faster than neat polymer, as can be observed in this study.

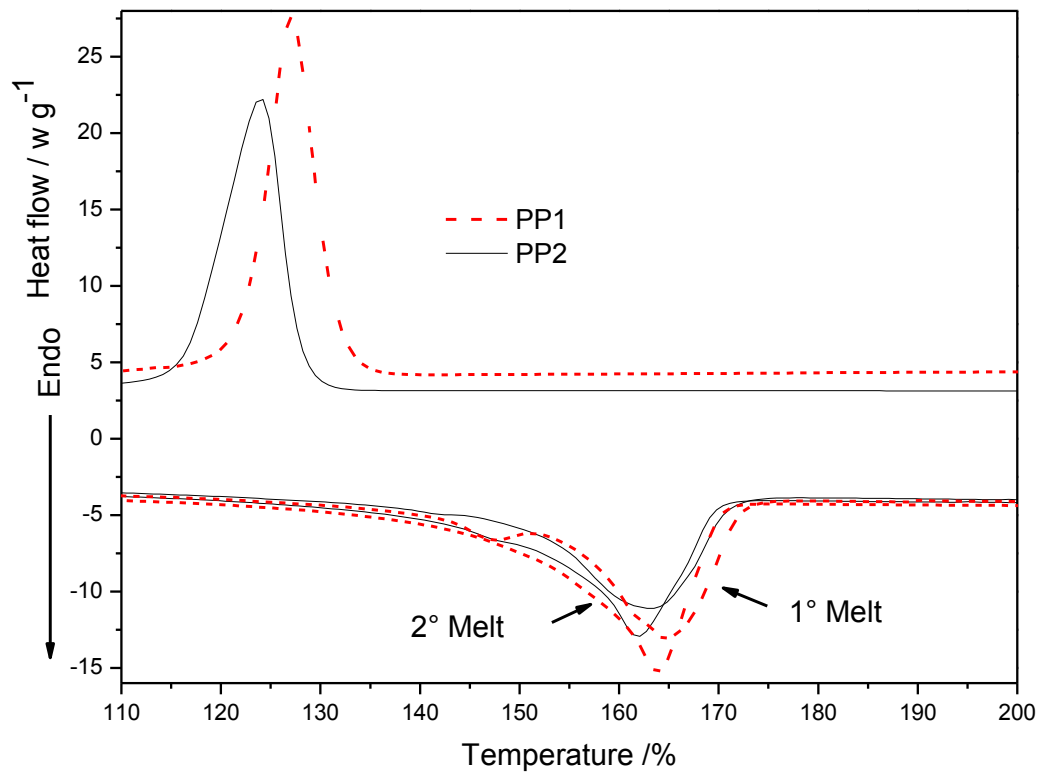


**Figure 3: DSC curves in the melting of PP1 and PP2.**

### 3.4. X-Ray diffraction

The X-Ray diffraction patterns of the samples are shown in Fig. 4.

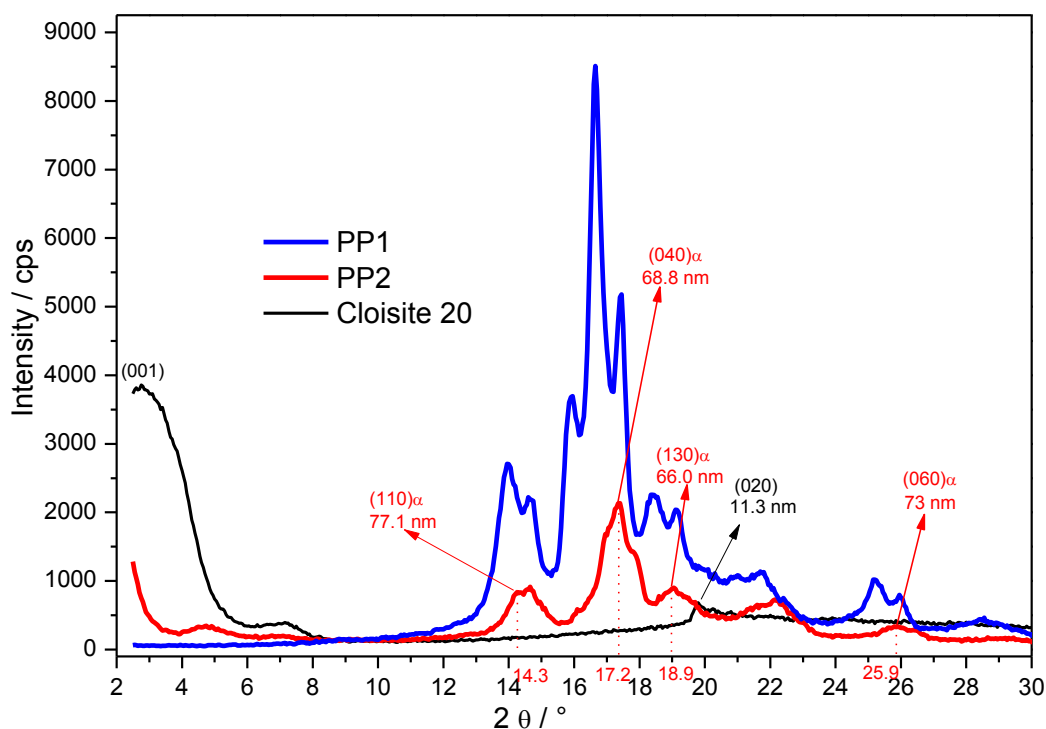


**Figure 4: X-ray diffraction pattern of PP1, PP2 and Cloisite.**

In Fig. 4, diffraction of PP structure was observed for. However, for PP2, there are clay peaks shifted, which means that polymer chains have been intercalated. According to the literature [24], the peak shift indicates that the gallery has expanded, and it is usually assumed that polymer chains have been intercalated into the gallery. It is possible that the gallery expansion may in some cases be caused by intercalation of oligomers or low molecular weight polymer chains. The literature seemed to suggest that “intercalation” would be useful and perhaps a precursor to exfoliation.

#### 4. CONCLUSIONS

The application of sonication during the preparation of PP nanocomposite showed interesting results. The scanning electron microscopy and dispersive spectroscopy images have shown an intense peak of Ag. DSC results revealed that introducing content of clay in PP films decreased the degree of crystallinity. PP2 have demonstrated an diffraction peak shift due to the intercalation. The antibacterial activities and their composites with polypropylene were tested against *Staphylococcus aureus* and *Escherichia coli*. However there has no biocidal effect in the polypropylene film.

#### ACKNOWLEDGEMENTS

This project was supported by CAPES. The authors are grateful to the Centre of science and technology of materials- CCTM/IPEN, for microscopy analysis (SEM), the technicians Mr.

Eleosmar Gasparin and Nelson R. Bueno, for technical support and multipurpose gamma irradiation facility at the CTR/IPEN.

## REFERENCES

1. S. Sanchez-Valdes, "Sonochemical deposition of silver nanoparticles on linear low density polyethylene/cyclo olefin copolymer blend films," *Polymer Bulletin*, **71**, pp.1611-1624 (2014).
2. Y. Dong, D. Bhattacharyya, P. J. Hunter, "Experimental characterization and object-oriented finite element modeling of polypropylene/organoclay nanocomposites," *Composites Science and Technology*, **68**, pp. 2864-2875 (2008).
3. W. Lertwimolnun, B. Vergnes, "Influence of compatibilizer and processing conditions on the dispersion of nanoclay in a polypropylene matrix," *Polymer*, **46**, pp.3462–3471 (2005).
4. M. Ataefard, S. Moradian, "Surface properties of polypropylene/organoclay nanocomposites," *Applied Surface Science*, **257**, pp.2320-2326 (2011).
5. W. L. Oliani, L. F. C. P. Lima, D. F. Parra, D. B. Dias, A. B. Lugao. "Study of the morphology, thermal and mechanical properties of irradiated isotactic polypropylene films," *Radiation Physics and Chemistry*, **79**, pp.325-328 (2010).
6. M. Keizo, C. Song, *Radiation Processing of Polymer Materials and Its Industrial Applications*, John Wiley & Sons, Inc., Hoboken & New Jersey (2012).
7. F. Hussain, M. Hojjati, M. Okamoto, R. E. Gorga, "Polymer-matrix nanocomposites, processing, manufacturing, and application: An overview," *Journal of Composite Materials*, **40**, pp.1511-1575 (2006).
8. L. Delva, K. Ragaert, J. Degrieck, L. Cardon, "The Effect of Multiple Extrusions on the Properties of Montmorillonite Filled Polypropylene," *Polymers*, **6**, pp. 2912-2927 (2014).
9. M. S. Wang, T. J. Pinnavaia, "Clay-Polymer Nanocomposites Formed from Acidic Derivatives of Montmorillonite and an Epoxy Resin," *Chemistry of Materials*, **6**, pp.468-474 (1994).
10. K. K. Goli, N. Gera, X. Liu, B. M. Rao, O. J. Rojas, J. Genzer, "Generation and Properties of Antibacterial Coatings Based on Electrostatic Attachment of Silver Nanoparticles to Protein-Coated Polypropylene Fibers," *Applied Materials & Interfaces*, **5**, pp.5298-5306 (2013).
11. R. Dastjerdi, M. Montazer, "A review on the application of inorganic nano-structured materials in the modification of textiles: Focus on anti-microbial properties," *Colloids and Surfaces B: Biointerfaces*, **79**, pp.5-18 (2010).
12. W. L. Oliani, D. F. Parra, L. F. C. P. Lima, N. Lincopan, A. B. Lugao, "Development of a nanocomposite of polypropylene with biocide action from silver nanoparticles," *Journal of applied polymer science*, **132**, 42218 (2015).
13. E. Fages, J. Pascual, O. Fenollar, D. Garcia-Sanoguera, R. Balart, "Study of Antibacterial Properties of Polypropylene Filled With Surfactant-Coated Silver Nanoparticles," *Polymer Engineering and Science*, **51**, pp.804-811 (2011).
14. S. H. Jeong, S. Y. Yeo, S. C. Yi, "The effect of filler particle size on the antibacterial properties of compounded polymer/silver fibers," *Journal Of Materials Science*, **40**, pp.5407-5411 (2005).
15. R. Foldbjerg, P. Olesen, M. Hougaard, D. A. Dang, H. J. Hoffmann, H. Autrup, "PVP-coated silver nanoparticles and silver ions induce reactive oxygen species, apoptosis and necrosis in THP-1 monocytes," *Toxicology Letters*, **190**, pp.156-162 (2009).



16. A. Akelah, A. Moet, "Polymer-clay nanocomposites: Free-radical grafting of polystyrene on to organophilic montmorillonite interlayers," *Journal of Materials Science*, **31**, pp.3589-3596 (1996).
17. G. Choudalakis, A. D. Gotsis, "Permeability of polymer/clay nanocomposites: A review," *European Polymer Journal*, **45**, pp.967-984 (2009).
18. P. Reichert, H. Nitz, S. Klinke, R. Brandsch, R. Thomann, R. Mülhaupt, "Poly(propylene)/organoclay nanocomposite formation: Influence of compatibilizer functionality and organoclay modification macromolecular," *Materials and Engineering*, **275**, pp.8-17 (2000).
19. W. L. Oliani, D. F. Parra, A. B. Lugao, "UV stability of HMS-PP (high melt strength polypropylene) obtained by radiation process," *Radiation Physics and Chemistry*, **79**, pp.383-387 (2010).
20. D. M. Fermino, D. F. Parra, W. L. Oliani, A. B. Lugao, F. R. V. Díaz, "HMSPP nanocomposite and Brazilian bentonite properties after gamma radiation exposure," *Radiation Physics and Chemistry*, **84**, pp.176-184 (2013).
21. JIS Z 2801:2010 (adapted). Japanese Industrial Standard. Antimicrobial Products - Test for antimicrobial activity and efficacy.
22. P. Roonasi, A. Holmgren, "A Fourier transform infrared (FTIR) and thermogravimetric analysis (TGA) study of oleate adsorbed on magnetite nanoparticles surface," *Applied Surface Science*, **255**, pp.5891-5895 (2009).
23. Q. Yuan, S. Awate, R.D.K. Misra, "Nonisothermal crystallization behavior of polypropylene clay nanocomposites," *European Polymer Journal*, **42**, pp.1994-2003 (2006).
24. D. R. Paul, L. M. Robeson, "Polymer nanotechnology: Nanocomposites," *Polymer*, **49**, pp.3187-3204 (2008).

